Thermolytic Conversion of Copper (II) Based Coordination Polymer into Copper Oxide–Carbon Nanocomposite for Selective Removal of Cd (II) from Aqueous Solution

Charles O. Oseghale, Elias E. Elemike, Ayi A. Ayi, Ayomide H. Labulo, Elijah T. Adesuji & Benjamin Orimolade

Journal of Cluster Science
Including Nanoclusters and Nanoparticles

ISSN 1040-7278

J Clust Sci
DOI 10.1007/s10876-020-01790-y

Springer

Your article is protected by copyright and all rights are held exclusively by Springer Science+Business Media, LLC, part of Springer Nature. This e-offprint is for personal use only and shall not be self-archived in electronic repositories. If you wish to self-archive your article, please use the accepted manuscript version for posting on your own website. You may further deposit the accepted manuscript version in any repository, provided it is only made publicly available 12 months after official publication or later and provided acknowledgement is given to the original source of publication and a link is inserted to the published article on Springer's website. The link must be accompanied by the following text: "The final publication is available at link.springer.com".

Author's personal copy

Journal of Cluster Science
https://doi.org/10.1007/s10876-020-01790-y

ORIGINAL PAPER

Thermolytic Conversion of Copper (II) Based Coordination Polymer into Copper Oxide–Carbon Nanocomposite for Selective Removal of Cd (II) from Aqueous Solution

Charles O. Oseghale[1] · Elias E. Elemike[2] · Ayi A. Ayi[3] · Ayomide H. Labulo[1] · Elijah T. Adesuji[4] · Benjamin Orimolade[5]

Received: 20 January 2020
© Springer Science+Business Media, LLC, part of Springer Nature 2020

Abstract

In this work, we report the synthesis of a Cu (II) based metal–organic frameworks (HKUST-1) by mechanochemical method and metal-oxide–carbon nanocomposite (CuO@C) as thermolysis products. The prepared HKUST-1 and composite were characterized by elemental CHNS/O microanalysis, scanning electron microscopy equipped with energy dispersive X-ray spectroscopy (SEM–EDX), transmission electron microscopy (TEM), ultraviolet–visible spectroscopy (UV–vis), thermogravimetric analyses (TGA), fourier-transform infrared spectroscopy (FTIR), powder X-ray diffraction (PXRD) and Brunauer–Emmett–Teller (BET) analysis. The TEM analysis, confirmed the CuO nanoparticles in the porous carbon matrix. The synthesized compounds were further investigated for adsorption of Cd (II) from aqueous solution. The composite exhibited a high cadmium uptake of 132.6 mg g^{-1} compared to the parent HKUST-1, and fast kinetics with a kinetic rate constant k_2 of 0.031 g mg^{-1} min^{-1}, which is greater than some existing adsorbents for cadmium adsorption from aqueous solution under similar condition. The cadmium adsorption on CuO@C composite showed pH, temperature and time dependence to the prepared HKUST-1, as well as greater surface area and pore volume. The CuO@C composite can be readily recycled and regenerated without significant loss of the cadmium adsorption capacity.

Keywords Metal–organic frameworks · Nanostructure · Adsorption · Metal-oxide–carbon · Composites

Introduction

In recent times, metal/metal oxide embedded in carbon matrix have demonstrated superior performances in various areas of applications such as adsorption, catalysis and gas sensing [1, 2]. Also, much attention has been drawn on the use of nanostructured porous carbon materials as sorbents in liquid adsorption, catalyst support and fuel cells [3, 4]. Nevertheless, the synthesis of metal oxide still suffers drawbacks, such as aggregation, which ultimately reduces their performances [4]. In order to improve their potential, the textural properties of these low surface area (non-porous) metal oxides may undergo significant changes upon their dispersion onto carbon matrices such as porous carbon, graphenes and carbon nanotubes [5–7]. The role of porous carbon materials is to modify their physical properties and to prevent the aggregation of nanoparticles [8].

Metal–organic frameworks are new types of hybrid materials that are constructed by metal ions or metal clusters and organic linkers. They are highly-crystalline

Electronic supplementary material The online version of this article (https://doi.org/10.1007/s10876-020-01790-y) contains supplementary material, which is available to authorized users.

✉ Elias E. Elemike
chemphilips@yahoo.com; elemike.elias@fupre.edu.ng

[1] Department of Chemistry, Federal University of Lafia, Lafia, Nigeria

[2] Department of Chemistry, Federal University of Petroleum Resources, Effurun, Nigeria

[3] Department of Chemistry, University of Calabar, Calabar, Nigeria

[4] Centro de Investigacion en Materiales Avanzados S.C. (CIMAV), Unidad Monterrey, Monterrey, Mexico

[5] Department of Chemistry, University of Ilorin, Ilorin, Nigeria

Published online: 01 April 2020

Author's personal copy

porous solids that have gained a great deal of research interest in the last decade [9, 10]. Due to their high porosities and tunable structural properties, they have wide applications including adsorption, catalysis and gas storage [11, 12]. Recently, metal–organic frameworks have been used as template materials and precursors for preparation of nano-porous carbon and nano-porous oxides [13, 14]. During thermal treatment of the MOFs under N_2 atmosphere, the organic linkers in the MOFs are transformed into carbon phases with highly-porous structural properties, which leads to the formation of metal-oxide carbon composites [15]. On the other hand, thermal treatment in the presence of air, converts the organic linkers (existing in the MOFs) to gaseous CO_2, leaving metal oxides behind [16].

Increase in industrial and mining activities are responsible for the presence of toxic pollutants such as heavy metal ions in aqueous system [17]. The discharge of untreated wastewater/effluents into the aquatic environment poses higher health risks to their dependents [18, 19]. Heavy metal ions are non-biodegradable and persistence in nature and thus, a variety of methods to achieve effective removal of Cd^{2+} from wastewater has been explored in the past [20, 21]. Among these methods, adsorption has been investigated extensively for the removal of Cd^{2+} from wastewater considering its facile regeneration, low cost, simple design and easy operations [22–24]. However, adsorbents like activated carbon suffer drawbacks ranging from low capacity, moderate affinity and low surface area for Cd^{2+} removal. The drawbacks associated with the existing sorbents led to the development of new porous and highly ordered hybrid materials, for efficient removal of Cd (II) from aqueous solutions. Metal–organic frameworks, a new class of porous materials have played a great role to this advantage.

In this study, interest is on the conversion of a Cu (II) based coordination polymer (HKUST-1) into a metal oxide–carbon nanostructured composite, by thermolysis at 800 °C under N_2 atmosphere. The aim is to prepare a highly active, stable and reusable adsorbent materials for the removal of Cd (II) from aqueous solution. This procedure is adopted in order to develop materials with enhanced properties.

Experimental

Materials and Reagents

The 1,3,5-benzenetricarboxylic acid (H_3BTC) ligand and high purity copper acetate monohydrate salt (98%) were purchased from BDH chemicals and used as received. All other chemicals, including the solvents, were of analytical grade and used as received. The cadmium stock solution of 0.01 mol dm^{-3} was prepared by dissolving 0.3085 g of Cd $(NO_3)_2{\cdot}4H_2O$ in 100 cm^3 of deionized water. The standard solutions of the Cd (II) were prepared by serial dilution of the original stock solution with deionized water.

Instrumental Measurements

The elemental CHNS/O microanalyses were carried out using Perkin–Elmer 240C series (USA) elemental analyzer whereas the infrared spectra were obtained within the range of (4000–400 cm^{-1}) using a SHIMADZU 8400C (Japan) Fourier transform spectrometer. Powder X-ray diffraction (PXRD) patterns were recorded on a Bruker D8 Advanced X-ray Diffractometer (Germany) under Cu–Kα radiation. The morphologies and sizes of the materials were studied using Hitachi S-4800 scanning electron microscope (SEM) and JEOL 1010 transmission electron microscope (TEM) instruments. The images were processed using an Image J (1.42q) software. The absorption spectra were recorded with a T-60 UV–visible spectrophotometer (USA) at a resolution of 1 nm, within the wavelength range of 200–800 nm and the cadmium concentration determined using A Zeenit 700 absorption spectrometer (Germany) coupled with a flame atomizer and a cadmium hollow cathode lamp. A quantachrome NOVA/4000 adsorption instrument, were used to determine the specific surface area (BET) with N_2 sorption at 77 K. Thermal behavior of the composites were analyzed on a TA instruments Q500 Thermogravimetric analyzer system (USA) with the sample held in a platinum pan under N_2 gas flow of 100 mL min^{-1} and heating rate of 25 °C min^{-1}.

Synthesis of HKUST-1 by Method of Ball-Milling

The mechanochemical synthesis was carried out in a conventional ball mill by adopting the procedure described by Pichon et al. [25], with little modification. Briefly, copper acetate monohydrate and 1,3,5-benzenetricarboxylic acid (molar ratio of 3:2) were introduced into a stainless-steel ball-mill closed vessel equipped with steel balls at room temperature for 20 min at a speed of 30 Hz. The products obtained were desolvated by heating at 150 °C for 45 min with 88% yield.

Synthesis of CuO@C Nanocomposite

The composite material was prepared by direct calcination of the precursor compound (HKUST-1). About 0.20 g of the HKUST-1 was weighed in an alumina crucible and placed into the reactor (Chemglass tubular reactor) for calcination. It was heated from 25 to 800 °C under N_2 atmosphere. The obtained black products (CuO@C) were cooled to room temperature and further characterized.

Author's personal copy

Adsorption Studies

The adsorption of Cd^{2+} from aqueous solution with the HKUST-1 and calcined composite were investigated using a batch equilibrium technique. In general, 25 cm^3 of known initial Cd^{2+} concentration was maintained at pH 6.0 by the addition of appropriate amount of 0.1 M NaOH and HNO_3 solutions. About 0.05 g of the adsorbent was added and then mounted on a shaker for at least 20 min to speed up the adsorption process. Physicochemical parameters such as initial metal ion concentration, effects of pH, temperature and contact time, were varied to maximize their adsorption and to obtain the adsorption isotherms. The amount of heavy metal ions adsorbed is reported by the removal efficiency in (%), as given thus:

$$Removal\ efficiency(\%) = \frac{C_i - C_e}{C_i} \times 100 \quad (1)$$

where C_i and C_e (mg L^{-1}) are the initial and final equilibrium concentrations of Cd^{2+} in the solution respectively.

Results and Discussion

Characterization of the MOFs and Copper Oxide Composite

The powder X-ray diffraction (PXRD) patterns of HKUST-1 and CuO@C composite are presented in Fig. 1. From Fig. 1b, the diffraction peaks at 2θ = 32.2°, 36.8°, 39.2°, 49.4°, 53.2°, 59.4°, 61.9°, 66.1°, 69.3°, 73.2° and 75.6° which corresponds to 110, 002, 111, 202, 020, 202, 113, 311, 220, 113 and 311 lattice planes can be assigned to the monoclinic crystalline CuO structure (JCPDS card no. 80-1917). However, the peak at 26.4° (002) was specifically due to carbon. The absence of additional peaks in the CuO@C composite spectra indicates its high purity [26]. Figure 1a, b show that, there was a significant change in structure upon calcination of HKUST-1 at 800 °C. The sharp peaks observed in the composite may be due to the high crystalline nature of the calcined products [26].

The FTIR spectra (Fig. 2) of the HKUST-1 showed broad bands at the range of 3446–3281 cm^{-1} [27]. However, the disappearance of these bands in the composite is due to total transformation of the organic linkers present in the HKUST-1 into carbon phases, leaving behind a highly porous nanostructured composite [15]. The bands at 532

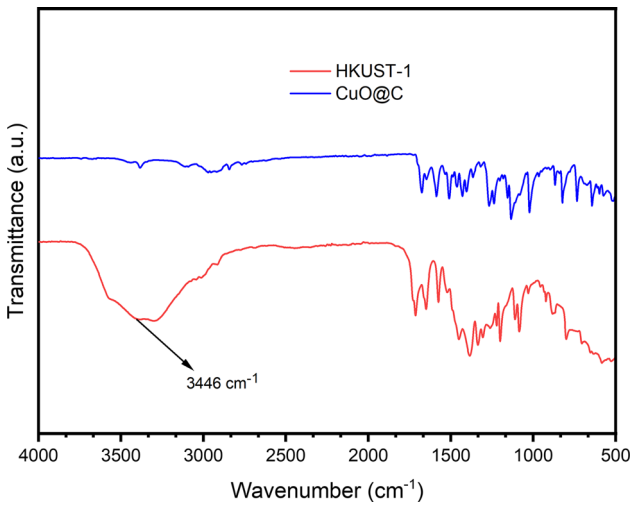

Fig. 2 FT-IR spectra of the HKUST-1 and CuO@C composite

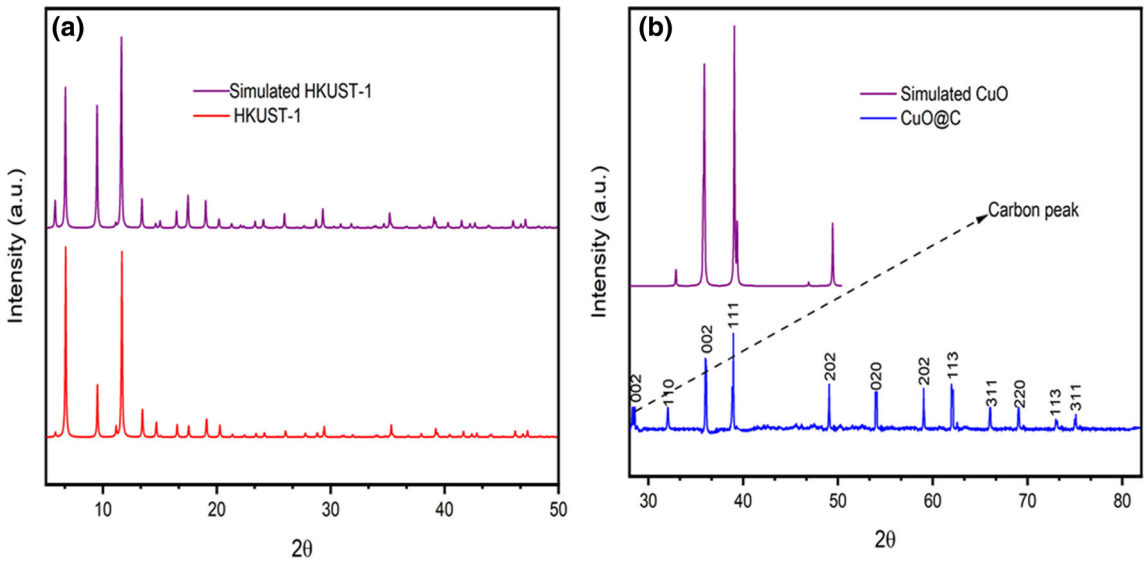

Fig. 1 PXRD patterns and comparison of the prepared and simulated **a** HKUST-1 and **b** CuO@C composite

Author's personal copy

and 643 cm^{-1}, further confirmed the presence of the stretching vibrations of the Cu metal in the nanomaterials. The SEM images were used to investigate the surface morphologies of the prepared HKUST-1 and composite. The materials displayed uniform (homogeneous) structure (Fig. 3a, c).

The TEM image and the particle size distribution chart, showing the average particle diameter (10.6 nm) of the CuO@C nanostructure are shown in Figs. 3d and 4 respectively. The nanoparticles Ferrets diameter were determined using an Image J software, by counting the particles on each image. The nanostructured composite showed slight agglomeration which may be attributed to the high heat treatment exceeding the threshold for effective stabilization of the particle size. The SEM–EDX spectra (see Supplementary Material Fig. S1), confirmed the presence of copper metal and oxygen at different percentages by weight of the prepared HKUST-1 and CuO@C composite respectively. The BET and Langmuir surface area with pore volumes of HKUST-1 and CuO@C were derived from nitrogen isotherms at 77 K and results are presented in Fig. S4 and Table S1 respectively. In comparison with the CuO@C (879 m^2 g^{-1}), the BET surface area of the MOFs was reduced to 692 m^2 g^{-1}. This could be due to the fact that the organic linkers in the HKUST-1 have been converted to carbon phases during the calcination process [15]. Thus, the porous properties of this calcined composite are better compared to the parent MOFs.

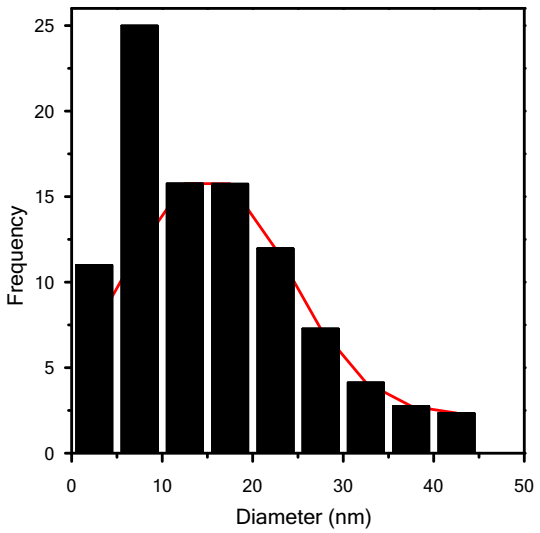

Fig. 4 Particle size distribution chart of CuO@C nanostructure composite

Thermal Stability of the Materials

The thermal decomposition of HKUST-1 and CuO@C nanostructured composites carried out under nitrogen atmosphere are presented in Fig. S2.

The percentage weight loss was monitored within the range of 20–1000 °C. As shown in the TG curves, weight loss of 3% between room temperature to 90 °C for HKUST-1, was due to desorption of water molecules from the porous framework structure. The second weight loss of

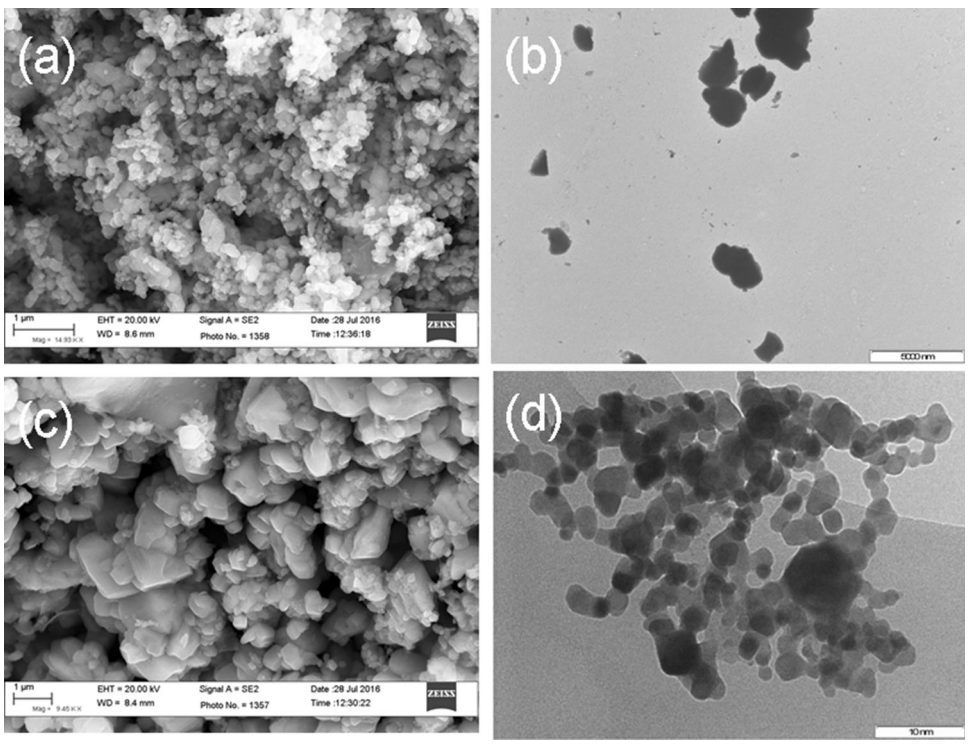

Fig. 3 SEM and TEM images of **a**, **b** HKUST-1 and **c**, **d** CuO@C

Author's personal copy

32% observed at 450 °C was ascribed to the decomposition of organic matter in the HKUST-1 structure. The CuO@C composite show good stability up to 900 °C before total decomposition.

Investigation of the Effects of pH, Temperature and Contact Time on Cadmium Adsorption

The cadmium adsorption was evaluated as a function of initial cadmium concentration (25–200 mg L^{-1}), at a pH of 6.0, 0.05 g adsorbent dose and 20 min contact time (Fig. 5a). The quantity of Cd^{2+} removed at equilibrium by the sorbents increased with an increase in initial metal ion concentration. An increase in the metal ion concentration does not correspond to enhanced removal of cadmium but a decline due to an increase in the driving force of the concentration gradient [28]. Figure 5b describes the influence of the pH on the adsorptive capacities and surface changes of the adsorbents [28]. The variation in pH shows that the optimum pH for the adsorption of Cd (II) is 6.0. The quantity adsorbed at equilibrium q_e (mg g^{-1}) improves with increasing pH from 3.0 to 6.0 for the HKUST-1 and the composite material. Such situation arises due to drop in competition between the proton [H^+] and the positively charged metal ion surface sites, resulting in a low repulsion of the adsorbing metal ion [29]. A further increase in pH values > 6.0, results in a gradual decrease of the adsorption capacity due to degree of protonation of the adsorbent functional groups [29]. Low amount of cadmium can be adsorbed due to the competition between protons and the cadmium ions in aqueous solution at pH < 3.0. The highest quantity adsorbed by CuO@C at a pH of 6.0 was achieved at 80.99% (Fig. 5b).

The increase in adsorption due to steady rise in temperature (Fig. 5c), may be due to diffusion control system, which is an endothermic process i.e. the rise in temperature

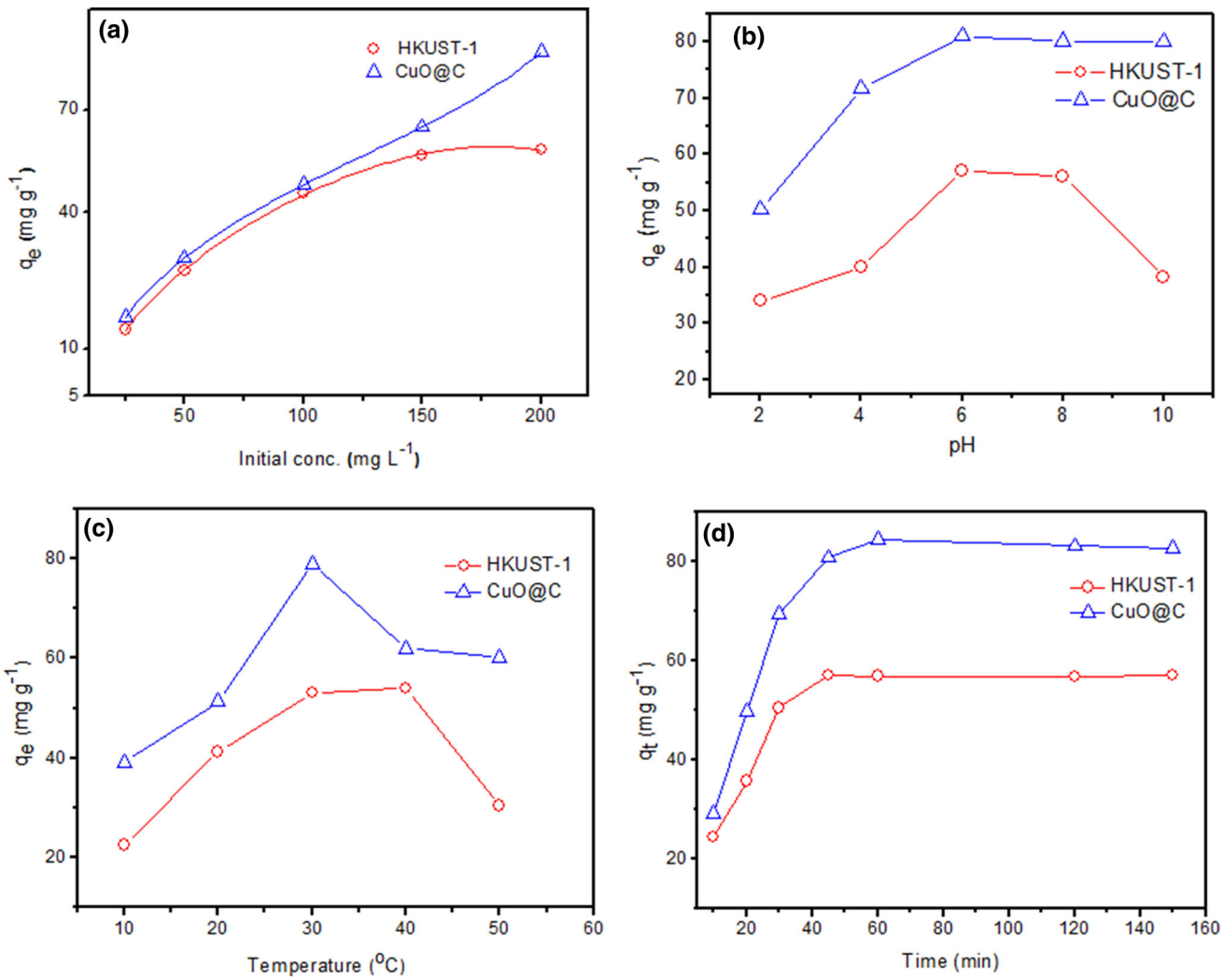

Fig. 5 Initial cadmium concentration (**a**) and effect of pH (**b**) temperature (**c**) time (**d**) of HKUST-1 and CuO@C

Author's personal copy

favors the transport of the metal ions within the pores of the adsorbent materials. The peak of adsorption was reached at 40 °C for the HKUST-1 and 30 °C for CuO@C composite. A further increase in the temperature led to gradual decrease of the metal ions adsorbed on the surface of the sorbents due to weakening of the forces between the sorbent materials and cadmium ions in the solution [28]. The metal ions escape from the surface of the sorbents at higher temperature into a solution phase is attributed to an increase in kinetic energy [28].

The importance of contact time significantly influences the identification of possible adsorption rate process of heavy metal ions uptake. In order to achieve the rapidness of binding and saturation uptake, the effect of contact time in adsorption of cadmium was studied within the range of 10–150 min, with 0.05 g of the adsorbents at cadmium concentration of 200 mg L^{-1} for CuO@C and 150 mg L^{-1} for the HKUST-1. In (Fig. 5d), the absorptivity of the Cd^{2+} on the sorbents increased with increase in contact time until equilibrium is reached at 60 min, with CuO@C uptake at 80.9% (Fig. S3). There was no change in the removal efficiency of cadmium after 60 min. The CuO@C composite showed a faster adsorption rate for Cd (II) ions in aqueous solution compared to the parent HKUST-1 and other adsorbents under similar conditions. Such improvement in adsorption could be due to the enhanced surface area and pore volume of the CuO@C nanocomposites [30, 31]. The contact time of 60 min was then selected for further investigations.

Cadmium Adsorption Isotherm

Adsorption isotherm was obtained using solutions containing different initial cadmium concentration ranging from 25 to 200 mg L^{-1}, to estimate the Cd (II) uptake capacity on the sorbents, under optimized experimental conditions of 60 min contact time, and pH of 6.0 as shown in Fig. 6. The Langmuir isotherm model described by Eq. 2 assumes that the solid surface-active sites can be occupied by a layer of adsorbate, since their active sites are independent [32].

$$\frac{C_e}{q_e} = \frac{C_e}{Q_m} + \frac{1}{Q_m K_l} \tag{2}$$

where C_e is the concentration at equilibrium in the solution (mg L^{-1}), q_e is the amount of Cd^{2+} adsorbed on the sorbents at equilibrium (mg g^{-1}), Q_m (mg g^{-1}) is the maximum adsorption capacity and K_L is the Langmuir constant (L mg^{-1}). The reciprocal of slope of the plot of C_e/q_e against Ce, can be used to obtain the maximum adsorption capacity (Q_m) at a monolayer coverage. The Langmuir constant K_L can be obtained from the intercept ($1/Q_m K_L$), which quantitatively reflects the affinity of binding sites to

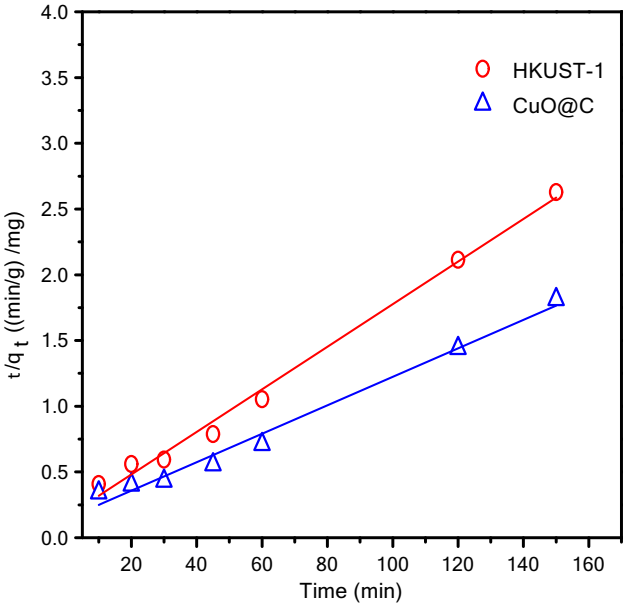

Fig. 6 Langmuir plot of HKUST-1 and CuO@C

the energy of adsorption. The Langmuir isotherm model was preferred in this work, since it gave a satisfactory fit to the experimental data and a higher R^2 values for the sorbents.

The CuO@C showed greater adsorption uptake to HKUST-1 (Fig. 6). The Langmuir plot was used to determine the maximum adsorption capacity (Q_m), [33] and the values are presented in Table S1. The composite (136.2 mg L^{-1}) showed a higher maximum uptake capacity better than HKUST-1 and other reported sorbents used for cadmium adsorption under similar conditions as summarized in Table S1. The higher uptake of Cd^{2+} in aqueous solution by the CuO@C composite was attributed to its high surface area and pore volumes.

Cadmium Adsorption Kinetics

Further study on the adsorption kinetics of Cd^{2+} on the adsorbents was carried out at initial cadmium concentration of 200 mg L^{-1} for CuO@C and 150 mg L^{-1} for HKUST-1 at a pH of 6.0. A pseudo-second-order linear kinetic model as shown in Eq. 3 was applied to obtain the linear plot in Fig. 7. Adsorption process of adsorbate depends on a blend of multiple mechanistic steps such as chemical reactions, mass transfer, diffusion control etc.

The pseudo-second-order kinetic model is described with the Eq. 3 below [33]:

$$lnq_e - q_t = ln(q_e) - k_i t \tag{3}$$

where q_e (mg g^{-1}) and q_t (mg g^{-1}) are the amounts of heavy metal ions (cadmium) adsorbed at equilibrium and at

Author's personal copy

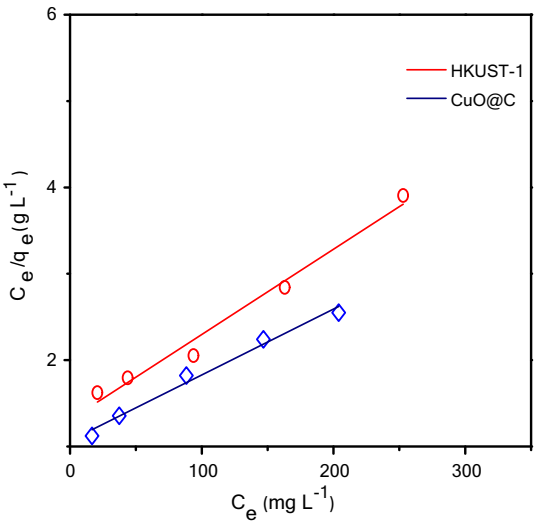

Fig. 7 Pseudo-second-order kinetics of HKUST-1 and CuO@C

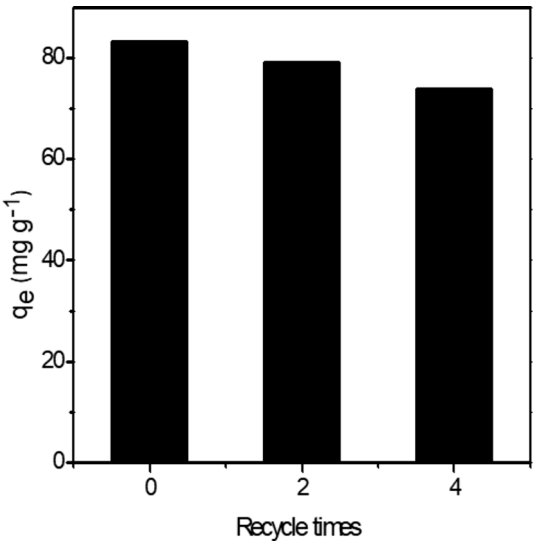

Fig. 9 Recyclability of CuO@C composite

time t (min) respectively; k_2 (g mg min^{-1}) is the pseudo-second-order kinetic rate constant.

The high correlation factors (r^2), indicate that the kinetic data obtained for the cadmium adsorption, are in good agreement and well fitted with the model. The value of 0.031 g mg^{-1} min^{-1} (Table S1), was calculated for the kinetic rate constant k_2, which is greater than some existing benchmark adsorbents for cadmium adsorption from aqueous solutions [34, 35].

Cadmium Desorption and Reusability of CuO@C

The powder X-ray diffraction and UV–vis analyses were used to monitor and confirm the structural integrity of the adsorbents as shown in Fig. 8a, b respectively. From the figures, it can be seen that the uptake capacity of the Cd^{2+} on CuO@C was gradually reduced after each cycle. This may be due to subsequent loss of the composite porosity after each desorption cycles. The CuO@C composite was easily regenerated by washing with 35 cm^3 of deionized water, and dried in an oven (70 °C) for 40 min before reuse. The CuO@C nanostructured composite retained more than 74% of its initial cadmium uptake capacity after a varied four cycle (Fig. 9).

Conclusion

The study successfully demonstrated the synthesis of copper nanostructured composite (CuO@C) by thermolysis of the synthesized copper (II) based MOF (HKUST-1) under N_2 atmosphere. The HKUST-1 and CuO@C composite were used for cadmium adsorption from aqueous solution. The CuO@C composite showed a maximum uptake of 132.6 mg g^{-1} compared to the parent HKUST-1, and fast kinetics with a kinetic rate constant k_2 of

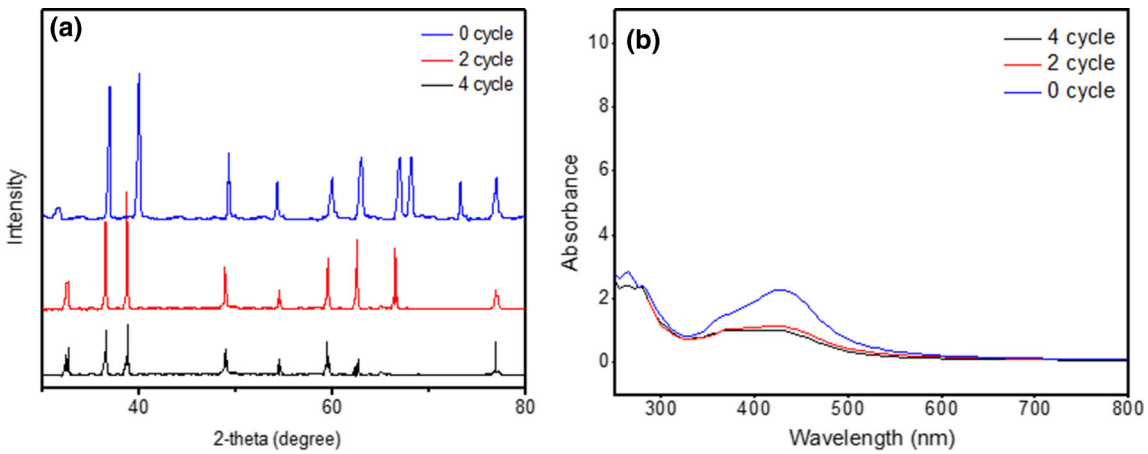

Fig. 8 PXRD patterns (**a**) and UV–vis (**b**) of CuO@C after 0, 2, 4 adsorption/elution cycles

Author's personal copy

0.031 g mg^{-1} min^{-1}, which is greater than some existing benchmark adsorbents for cadmium adsorption from aqueous solution under similar conditions. The higher uptake of cadmium on the composite could be attributed to its high surface area and synergistic effect of the well-dispersed and small-sized metal oxide nanoparticles embedded within the porous carbon matrix. Also, a favorable adsorption of the Cd (II) ions was achieved at a pH of 6.0. In addition, the composite can be readily recycled and regenerated without significant loss of the cadmium adsorption capacity. The preparation of the CuO@C nanostructured composite with the synthesized HKUST-1 as a precursor, paves way for efficient cadmium removal and other heavy metal ions from wastewater.

Acknowledgements We are grateful to the School of Chemistry, University of KwaZulu-Natal, Durban, South Africa for spectroscopy analyses.

Compliance with Ethical Standards

Conflict of interest The authors declare no conflict of interest.

References

1. Y. Shen (2015). *J. Mater. Chem. A.* **3**, 13188.
2. W. Yao, C. Shen, and Y. Lu (2013). *Compos. Sci. Technol.* **87**, 13.
3. S. Flandrois and B. Simon (1999). *Carbon N. Y.* **37**, 180.
4. Z. Hu, M. P. Srinivasan, and Y. Ni (2000). *Adv. Mater.* **12**, 65.
5. X. Tong, Y. Qin, and X. Guo (2012). *Small* **8**, 3395.
6. X. Sun (2003). *J. Dispers. Sci. Technol.* **24**, 567.
7. T.-H. Kim, K.-B. Lee, and J.-W. Choi (2013). *Biomaterials* **34**, 8670.
8. S. Miyanaga, H. Yasuda, and A. Hiwara (1990). *J. Macromol. Sci.* **27**, 1361.
9. G. Férey (2008). *Chem. Soc. Rev.* **37**, 214.
10. S. H. Jhung, N. A. Khan, and Z. Hasan (2012). *CrystEngComm* **14**, 7109.
11. J.-J. Chen, Y.-T. Chen, and D. S. Raja (2015). *Sci. Technol. Adv. Mater.* **16**, 54203.
12. J. Liu, L. Chen, and H. Cui (2014). *Chem. Soc. Rev.* **43**, 6061.
13. W. Chaikittisilp, K. Ariga, and Y. Yamauchi (2013). *J. Mater. Chem. A* **1**, 19.
14. J.-K. Sun and Q. Xu (2014). *Energy Environ. Sci.* **7**, 2100.
15. H. Yue, Z. Shi, and Q. Wang (2014). *ACS Appl. Mater. Interfaces* **6**, 17074.
16. X. Yan, N. Lu, and B. Fan (2015). *CrystEngComm* **17**, 6433.
17. Z. Feng, S. Zhu, and D. R. Martins de Godoi (2012). *Anal. Chem.* **84**, 3770.
18. M. P. Waalkes (2000). *J. Inorg. Biochem.* **79**, 244.
19. M. Xu, P. Hadi, G. Chen, and G. McKay (2014). *J. Hazard. Mater.* **273**, 123.
20. M. E. Clares, M. G. Guerrero, and M. García-González (2015). *Int. J. Environ. Sci. Technol.* **12**, 1798.
21. Y. Ge, D. Xiao, Z. Li, and X. Cui (2014). *J. Mater. Chem. A* **2**, 2145.
22. S. S. Gupta and K. G. Bhattacharyya (2012). *Phys. Chem. Chem. Phys.* **14**, 6723.
23. Y. Wang, G. Ye, and H. Chen (2015). *J. Mater. Chem. A* **3**, 15298.
24. H.-T. Fan, J.-X. Liu, and H. Yao (2014). *Ind. Eng. Chem. Res.* **53**, 378.
25. A. Pichon, A. Lazuen-Garay, and S. L. James (2006). *CrystEngComm* **8**, 214.
26. A. El-Trass, H. ElShamy, I. El-Mehasseb, and M. El-Kemary (2012). *Appl. Surf. Sci.* **258**, 3001.
27. J.-J. Chen, Y.-T. Chen, and D. S. Raja (2015). *Materials* **8**, 5347.
28. R. Qadeer and S. Akhtar (2005). *Turk. J. Chem.* **29**, 100.
29. M. Ajmal, R. A. K. Rao, R. Ahmad, and J. Ahmad (2000). *J. Hazard. Mater.* **79**, 131.
30. F. Ge, M.-M. Li, H. Ye, and B.-X. Zhao (2012). *J. Hazard. Mater.* **211**, 372.
31. F. A. B. Silva and F. L. Pissetti (2014). *J. Colloid Interfaces Sci.* **416**, 100.
32. I. Langmuir (1918). *J. Am. Chem. Soc.* **40**, 1403.
33. Z. Hasan, N. A. Khan, and S. H. Jhung (2016). *Chem. Eng. J.* **284**, 1413.
34. A. Dubey, A. Mishra, and S. Singhal (2014). *Int. J. Environ. Sci. Technol.* **11**, 1050.
35. X. Weng, S. Lin, Y. Zhong, and Z. Chen (2013). *Chem. Eng. J.* **229**, 34.

Publisher's Note Springer Nature remains neutral with regard to jurisdictional claims in published maps and institutional affiliations.